


PAPER

New and improved bounds on the contextuality degree of multi-qubit configurations

Axel Muller¹ , Metod Saniga² , Alain Giorgetti¹ , Henri de Boutray³, Frédéric Holweck^{4,5}

¹Université de Franche-Comté, CNRS, institut FEMTO-ST, F-25000 Besançon, France ²Astronomical Institute of the Slovak Academy of Sciences, 059 60 Tatranska Lomnica, Slovakia ³ColibriITD, France ⁴ICB, UMR 6303, CNRS, University of Technology of Belfort-Montbéliard, UTBM, 90010 Belfort, France ⁵Department of Mathematics and Statistics, Auburn University, Auburn, AL, USA

Corresponding author: Axel Muller; Email: axel.muller@femto-st.fr

(Received 04 October 2023; revised 07 February 2024; accepted 08 February 2024; first published online 18 April 2024)

Abstract

We present algorithms and a C code to reveal quantum contextuality and evaluate the contextuality degree (a way to quantify contextuality) for a variety of point-line geometries located in binary symplectic polar spaces of small rank. With this code we were not only able to recover, in a more efficient way, all the results of a recent paper by de Boutray et al. [(2022). *Journal of Physics A: Mathematical and Theoretical* 55 475301], but also arrived at a bunch of new noteworthy results. The paper first describes the algorithms and the C code. Then it illustrates its power on a number of subspaces of symplectic polar spaces whose rank ranges from 2 to 7. The most interesting new results include: (i) non-contextuality of configurations whose contexts are subspaces of dimension 2 and higher, (ii) non-existence of negative subspaces of dimension 3 and higher, (iii) considerably improved bounds for the contextuality degree of both elliptic and hyperbolic quadrics for rank 4, as well as for a particular subgeometry of the three-qubit space whose contexts are the lines of this space, (iv) proof for the non-contextuality of perpsets and, last but not least, (v) contextual nature of a distinguished subgeometry of a multi-qubit doily, called a two-spread, and computation of its contextuality degree. Finally, in the three-qubit polar space we correct and improve the contextuality degree of the full configuration and also describe finite geometric configurations formed by unsatisfiable/invalid constraints for both types of quadrics as well as for the geometry whose contexts are all 315 lines of the space.

Keywords: quantum geometry; multi-qubit observables; quantum contextuality; contextuality degree

1. Introduction

Quantum contextuality (see, e.g., Budroni et al. (2022) for a recent comprehensive review) is an important property of quantum mechanics saying that measurements of quantum observables cannot be regarded as revealing certain preexisting values; slightly rephrased, the result of a measurement depends on the context to which it is associated with. One of the simplest proofs of contextuality of quantum mechanics is the so-called Mermin–Peres square (Mermin, 1993; Peres, 1990), which demonstrates that already in the Hilbert space of two qubits it is not possible to consistently assign certain preexisting values to all observables. Another well-known (observable-based) contextuality proof is furnished by a Mermin pentagram (Mermin, 1993) living in the three-qubit Hilbert space. It is interesting to realize that both the Mermin–Peres square and the

Mermin pentagram are related to distinguished subgeometries of the symplectic polar spaces $\mathscr{W}(2N - 1, 2)$ associated with corresponding generalized N -qubit Pauli groups: the former being isomorphic to a geometric hyperplane of $\mathscr{W}(3, 2)$ (Saniga et al., 2007) and the latter living in a doily-related pentad of Fano planes of $\mathscr{W}(5, 2)$ (Lévay and Szabó, 2017; Saniga, 2021). These two and several other (e.g., Planat et al. (2013); Saniga and Lévay (2012)) geometrical observations have recently prompted us (de Boutray et al., 2022) to have a more systematic look at such geometrically backed quantum contextual configurations (i.e., sets of contexts) of $\mathscr{W}(2N - 1, 2)$ for some small values of N . This paper can be regarded as an organic continuation of de Boutray et al. (2022) with substantially improved algorithms and a more efficient code to address contextuality issues not only for all the types of geometric hyperplanes but also for a great number of subspaces of varying dimensions found in multi-qubit symplectic spaces of rank up to 7.

The paper is organized as follows. Section 2 summarizes the most essential properties of binary symplectic polar spaces and their relation with the generalized N -qubit Pauli groups and then recalls the definition of the degree of contextuality for a quantum configuration. Our contributions begin with Section 3 that presents algorithms and programs that we created to generate quantum configurations and reveal their contextuality or evaluate their degree of contextuality. In particular, we describe in detail two new algorithms to generate totally isotropic subspaces and to compute the degree of contextuality using a SAT solver. The main computational outcomes of our work are gathered in Section 4. Section 5 then establishes or discusses some general facts based on our findings. Here, we notably prove that there are no negative subspaces of dimension 3 and higher, introduce a new doily-based contextual configuration – the so-called two-spread – and compute its contextuality degree and, last but not least, we show that the contextuality degree of the configuration comprising all 315 three-qubit lines is 63, which is much lower than the previously known value. Section 6 concludes the paper with some open questions and an outline of prospective tasks.

2. Background

In this section, we collect all the necessary concepts and introduce the symbols and notation to the extent to make the paper as self-contained as possible so that the reader should be able to follow the main line of our reasoning without the urgent need to consult relevant references (like (Saniga et al., 2021, Section 2) and (Muller et al., 2022, Introduction)). For all integers $0 \leq k \leq 2N$, the $2N$ -dimensional vector space \mathbb{F}_2^{2N} over the 2-element field $\mathbb{F}_2 = (\{0, 1\}, +, \times)$ has vector subspaces of dimension k . Among them, the ones that are totally isotropic, without their 0, form the *symplectic space* $\mathscr{W}(2N - 1, 2)$, whose name is shortened as W_N . A subspace is *totally isotropic* if any two vectors x and y in it are mutually orthogonal ($\langle x|y \rangle = 0$), for the symplectic form $\langle \cdot | \cdot \rangle$ defined by:

$$\langle x|y \rangle = x_1y_{N+1} + x_{N+1}y_1 + x_2y_{N+2} + x_{N+2}y_2 + \dots + x_Ny_{2N} + x_{2N}y_N. \tag{1}$$

In other words, a (totally isotropic) subspace of W_N of (projective) dimension $1 \leq k \leq N - 1$ is a totally isotropic vector subspace of \mathbb{F}_2^{2N} of dimension $k + 1$ without its zero vector. A *point* of W_N is the unique element of a (totally isotropic) subspace of W_N of (projective) dimension 0. A *line* of W_N is a (totally isotropic) subspace of W_N of (projective) dimension 1. A *generator* of W_N is a (totally isotropic) subspace of W_N of (projective) dimension $N - 1$.

It is known that for a symplectic polar space $\mathscr{W}(2N - 1, q)$ embedded in a projective space $PG(2N - 1, q)$, the number of its k -dimensional subspaces is given by (see, e.g., (De Boeck et al., 2019, Lemma 2.10)):

$$\begin{bmatrix} N \\ k + 1 \end{bmatrix}_q \prod_{i=1}^{k+1} (q^{N+1-i} + 1), \tag{2}$$

where

$$\begin{bmatrix} n \\ k \end{bmatrix}_q = \prod_{i=1}^k \frac{q^{n-k+i} - 1}{q^i - 1} = \frac{(q^n - 1) \dots (q^{n-k+1} - 1)}{(q^k - 1) \dots (q - 1)}, \tag{3}$$

is the Gaussian (binomial) coefficient.

Let

$$X = \begin{pmatrix} 0 & 1 \\ 1 & 0 \end{pmatrix}, \quad Y = \begin{pmatrix} 0 & -i \\ i & 0 \end{pmatrix} \quad \text{and} \quad Z = \begin{pmatrix} 1 & 0 \\ 0 & -1 \end{pmatrix},$$

be the Pauli matrices, I the identity matrix, “ \otimes ” the tensor product of matrices, and $I^{\otimes N} \equiv I_{(1)} \otimes I_{(2)} \otimes \dots \otimes I_{(N)}$. From here on, all tensor products of observables $G_1 \otimes G_2 \otimes \dots \otimes G_N$ are called N -qubit observables and denoted $G_1 G_2 \dots G_N$, by omitting the symbol \otimes for the tensor product. Let “ \cdot ” denote the matrix product and M^2 denote $M \cdot M$. It is easy to check that $X^2 = Y^2 = Z^2 = I$, $X \cdot Y = iZ = -Y \cdot X$, $Y \cdot Z = iX = -Z \cdot Y$, and $Z \cdot X = iY = -X \cdot Z$. The N -qubit observables and the multiplicative factors ± 1 and $\pm i$, called *phase*, form the (generalized) (N -qubit) Pauli group $\mathcal{P}^{\otimes N} = (\{1, -1, i, -i\} \times \{I, X, Y, Z\}^{\otimes N}, \cdot)$.

The N -qubit observable $G_1 G_2 \dots G_N$, with $G_j \in \{I, X, Y, Z\}$ for $j \in \{1, 2, \dots, N\}$, is bijectively represented by the bitvector $(g_1, g_2, \dots, g_{2N})$ such that $G_j \leftrightarrow (g_j, g_{j+N})$ for $j \in \{1, 2, \dots, N\}$, with the assumption that $I \leftrightarrow (0, 0)$, $X \leftrightarrow (0, 1)$, $Y \leftrightarrow (1, 1)$ and $Z \leftrightarrow (1, 0)$.

The non-zero bitvectors are the points of W_N , and two observables commute if and only if their encodings are orthogonal. Therefore, we sometimes write that two points of W_N “commute.”

The *perpset* of the point $p \in W_N$ is the point-line geometry whose points are all points q which commute with p ($\langle p|q \rangle = 0$) and whose lines are all the lines of W_N which contain p (and thus contain only points in the perpset).

A *quantum configuration* is a pair (O, C) where O is a finite set of observables and C is a finite set of subsets of O , called *contexts*, such that (i) each observable $M \in O$ satisfies $M^2 = I^{\otimes N}$ (so, its eigenvalues are in $\{-1, 1\}$); (ii) any two observables M and M' in the same context commute, that is, $M \cdot M' = M' \cdot M$; (iii) the product of all observables in each context is either $I^{\otimes N}$ (*positive* context) or $-I^{\otimes N}$ (*negative* context). This sign is encoded by the *context valuation* $e : C \rightarrow \{-1, 1\}$ of (O, C) , defined by $e(c) = 1$ if the context c is positive, and $e(c) = -1$ if it is negative.

The points and lines of W_2 form a noticeable quantum configuration called the *two-qubit doily*. A N -qubit doily is a quantum configuration of W_N isomorphic to the two-qubit doily. A *spread of generators* is a set of pairwise disjoint generators that partition the set of points of W_N . A *two-spread* is a quantum configuration obtained by removing from a multi-qubit doily one spread of its lines, while keeping all its points.

2.1 Contextuality degree

Since the contextuality degree is the central subject of the present paper, this section recalls its definition and its connection with the phenomenon of quantum contextuality, both introduced in a former work (de Boutray et al., 2022).

Let (O, C) be a quantum configuration with $p = |O|$ observables $\{M_1, \dots, M_p\}$ and $l = |C|$ contexts $\{c_1, \dots, c_l\}$. Its *incidence matrix* $A \in \mathbb{F}_2^{l \times p}$ is defined by $A_{ij} = 1$ if the i -th context c_i contains the j -th observable M_j . Otherwise, $A_{ij} = 0$. Its *valuation vector* $E \in \mathbb{F}_2^l$ is defined by $E_i = 0$ if $e(c_i) = 1$ and $E_i = 1$ if $e(c_i) = -1$, where e is the context valuation of (O, C) .

With these notations, the quantum configuration (O, C) is contextual iff the linear system

$$Ax = E, \tag{4}$$

has no solution in \mathbb{F}_2^p . To be non-contextual means there is a solution $x \in \mathbb{F}_2^l$ that satisfies (4). Such a solution x can be thought of as a set of predefined values for the observables of O that satisfies all constraints imposed by the contexts of the configuration. Note that the predefined values defined by x do not depend on the contexts. When such a solution x exists, one says that there exists a Non-Contextual Hidden Variables (NCHV) model that reproduces the outcomes of the configuration predicted by quantum mechanics (Budroni et al., 2022; de Boutray et al., 2022).

In this setting, one can measure how much contextual a given quantum configuration is. Let us denote by $\text{Im}(A)$ the image of the matrix A as a linear map $A : \mathbb{F}_2^p \rightarrow \mathbb{F}_2^l$. Then, if (O, C) is contextual, necessarily $E \notin \text{Im}(A)$. A natural measure is the degree of contextuality (de Boutray et al., 2022), defined as follows:

Definition 1 (Contextuality degree). *Let (O, C) be a contextual configuration with the valuation vector $E \in \mathbb{F}_2^l$. Let us denote by d_H the Hamming distance on the vector space \mathbb{F}_2^l . Then one defines the degree d of contextuality of (O, C) by:*

$$d = d_H(E, \text{Im}(A)). \tag{5}$$

The notion of degree of contextuality measures in some sense how far a given configuration is from being satisfied by an NCHV model. The Hamming distance tells us what is the minimal number of constraints on the contexts that one should change to make the configuration valid by a deterministic function. In other words, $l - d$ measures the maximum number of constraints of the contextual configuration that can be satisfied by an NCHV model.

The degree of contextuality has also a concrete application as it can be used to calculate the upper bound for contextual inequalities. Let us consider a contextual configuration (O, C) and let us denote by C^+ the subset of positive contexts, C^- the subset of negative ones and by $\langle c \rangle$ the expectation for an experiment corresponding to the context c . The following inequality was established by Cabello (2010):

$$\sum_{c \in C^+} \langle c \rangle - \sum_{c \in C^-} \langle c \rangle \leq b. \tag{6}$$

Under the assumption of quantum mechanics, the upper bound b is the number of contexts of (O, C) , that is, $b = l$. However, this upper bound is lower for contextual configurations under the hypothesis of an NCHV model. Indeed, as shown in Cabello (2010), this bound is $b = 2s - l$, where s is the maximum number of constraints of the configuration that can be satisfied by an NCHV model. It connects the notion of degree of contextuality with the upper bound b :

$$b = l - 2d. \tag{7}$$

3. Methodology

This section details the algorithms and programs that we propose to generate quantum configurations and evaluate their degree of contextuality. All our programs are written in C language because it is faster and more accessible than the Magma language of the previous implementation (de Boutray et al., 2022). The algorithm for generating perpsets and hyperbolic and elliptic quadrics is presented in de Boutray et al. (2022), but we now implement it in C language. This algorithm consists of first generating all the lines and then selecting among them the ones belonging to a given perpsset or quadric.

For the generation of totally isotropic subspaces, including lines and generators, we propose a more efficient algorithm than in de Boutray et al. (2022), detailed in Section 3.1. The approach we propose to check contextuality (Section 3.3) and compute the contextuality degree (Section 3.2) is to use a SAT solver.

3.1 Generation of totally isotropic subspaces

Algorithm 1 presents the recursive function `TOTALLYISOTROPICSUBSPACES(N, k)` that generates the configuration of the points of W_N whose contexts are all the totally isotropic subspaces of dimension k of W_N , for $N \geq 2$ and $1 \leq k \leq N - 1$. Thus, the function call `TOTALLYISOTROPICSUBSPACES(N, N - 1)` builds the generators of W_N , and the function call `TOTALLYISOTROPICSUBSPACES(N, 1)` builds the configuration of W_N whose contexts are the lines of W_N .

The parameters $S = \{\}$ and $l = 0$ with a default value are only useful for the recursive calls and do not have to be specified when calling the function. The default values mean that calling `TOTALLYISOTROPICSUBSPACES(N, k)` automatically initializes S with the empty set and l with 0. The subsequent recursive calls will then assign different values to S and l .

Algorithm 1 Totally isotropic subspaces building algorithm.

```

1: function TOTALLYISOTROPICSUBSPACES( $N, k, S = \{\}, l = 0$ )
2:   if  $l = k + 1$  then return  $\{S\}$  end if;
3:    $T \leftarrow \{\}$ ;
4:   for each  $p > \max(S)$  in  $W_N$  do
5:      $C \leftarrow S \cup \{p\}$ ;
6:      $valid \leftarrow true$ ;
7:     for each  $q \in S$  do
8:       if  $\langle p|q \rangle = 1$  or  $p + q < p$  then  $valid \leftarrow false$ ; break end if;
9:        $C \leftarrow C \cup \{p + q\}$ 
10:    end for;
11:    if  $valid$  then  $T \leftarrow T \cup \text{TOTALLYISOTROPICSUBSPACES}(N, k, C, l + 1)$  end if
12:  end for;
13:  return  $T$ 
14: end function

```

The strict total order $<$ on points used in this algorithm is the lexicographic order, when points are considered as bitvectors (of even length). The expression $\max(S)$ represents the point p in S such that $\forall q \in S, p \geq q$. For the case of the empty set, it is assumed that $p > \max(\{\})$ holds for all p in W_N . Let us denote by $S + p$ the set $\{q + p \mid q \in S\}$ for any point p and any set of points S .

The following definition and facts justify some expected properties of the algorithm.

The *effective size* $t(p)$ of a point p is the size of the associated vector when we remove all the 0's from the beginning. For instance, $t((0, 0, 0, 0, 0, 1, 0, 1)) = t((1, 0, 1)) = 3$.

Let B be a basis of the subspace S (of dimension $l - 1$) at the beginning of the function. When $valid$ is true on Line 11, the variable C stores the subspace $S \cup \{p\} \cup (S + p)$, of dimension l . One of its bases is $B \cup \{p\}$. So, the algorithm is correct.

Conversely, let C be any totally isotropic subspace of dimension l . Let t be the maximal effective size of the elements of C . Let S be the subset of the elements of C whose effective size is strictly less than t . Let m be the minimal point of C whose effective size is t . Then, C will be built on Line 11 by the function call `TOTALLYISOTROPICSUBSPACES(N, k, S, l - 1)`, when the value of p on Line 4 is m . This remark justifies that the algorithm is complete and does not generate duplicates of the same subspace.

3.2 Computing the contextuality degree with a SAT solver

This section shows how the problem of finding the contextuality degree of a configuration can be reduced to a 3-SAT problem and thus take advantage of the numerous optimizations implemented

<p>(a)</p> $v_1 + v_2 + v_3 = 0$ $v_4 + v_5 + v_6 = 0$ $v_7 + v_8 + v_9 = 0$ $v_1 + v_4 + v_7 = 0$ $v_2 + v_5 + v_8 = 0$ $v_3 + v_6 + v_9 = 1$ <p>linear system</p>	<p>(b)</p> <pre> BC1.1 ASSIGN [5, 6] (v1 ^ v2 ^ v3 == F, v4 ^ v5 ^ v6 == F, v7 ^ v8 ^ v9 == F, v1 ^ v4 ^ v7 == F, v2 ^ v5 ^ v8 == F, v3 ^ v6 ^ v9 == T); </pre> <p>bc2cnf translation</p>
---	---

Figure 1. (a) Contextuality linear system for a Mermin–Peres square and (b) the corresponding bc2cnf file to decide whether 5 to 6 out of the 6 constraints can be solved (i.e., the contextuality degree is at most 1).

in the current SAT solvers. More precisely, we limit the effort of reduction to 3-SAT by going through an intermediary translation into the rich input language of the tool bc2cnf (Junttila and Niemelä, 2000), which creates itself a file in DIMACS format (suffix .cnf), the default format for SAT solvers.

The linear system $Ax = E$ is a set of equations in \mathbb{F}_2 (see the example for a Mermin–Peres square in Figure 1a, where + is the “exclusive or” symbol for exclusive disjunction). Each equation corresponds to a context of the configuration, with the expected value on the right-hand side. Since there are only zeros and ones, we rephrase the problem of knowing whether a configuration is contextual as finding a set of Boolean variables v_i ($1 \leq i \leq 9$ in Figure 1a) such that the exclusive disjunction of the variables is 0 for each positive context and 1 for each negative context. We can then use any SAT solver to compute a degree of contextuality, by using a feature of bc2cnf which allows us to specify bounds for the number of constraints that have to be satisfied.

A bc2cnf input (see an example in Figure 1b) mainly consists of constraints. The exclusive disjunction is represented by ^, the true and false values, respectively, by T and F, and the equality of expressions by ==. After the prefix BC1.1 specifying the version, the ASSIGN clause encapsulates the constraints under the form [low, high] (formula) where low and high, respectively, are the lower and upper bounds for the number of constraints to satisfy. After some experimentations, we found that kissat_gb (Chowdhury et al., 2021) was the fastest SAT solver for these kinds of systems.

Algorithm 2 Algorithm for calculating the degree of contextuality of a configuration C .

```

1: function CONTEXTUALITYDEGREE( $C$ )
2:    $i \leftarrow |C^+|$ ;
3:   while  $i < |C|$  do
4:      $sol \leftarrow sat\_sol(i + 1, |C|, C)$ ;
5:     if  $sol = \emptyset$  then return  $|C| - i$  end if;
6:      $i \leftarrow n\_match(sol, C)$ 
7:   end while;
8:   return 0
9: end function
    
```

The Algorithm 2 computes the contextuality degree of any configuration. The variable C is the set of the constraints of a configuration, the integer i is the current maximal known number of satisfiable constraints, and sol stores a solution for the set of constraints. The sat_sol function called on Line 4 is such that $sat_sol(i, j, C)$ retrieves a solution satisfying at least i and at most j of

the constraints in the set C . The $n_match(sol, l)$ returns the number of constraints of sol that are satisfied by l .

Let $|C^+|$ denote the number of positive constraints. We know that we can at least satisfy this number of constraints, by assigning the value 0 to all variables in C . For every iteration of the loop, we know that at least i constraints can be satisfied, so on Line 4 we ask the solver if at least one more constraint than i can be satisfied. If yes, we retrieve a solution sol of the SAT solver and then count the number of satisfied constraints, which can be more than $i + 1$. This number is then used as the new limit i until no solution can be found, which means that $|C| - i$ is the minimal number of unsatisfiable constraints in the system, that is, the contextuality degree of the corresponding configuration.

3.3 Checking contextuality with a SAT solver

When computing the contextuality degree is too time-consuming, we simply check contextuality. Checking contextuality of a quantum configuration is showing that a linear system $Ax = E$ has no solution in \mathbb{F}_2^p , for a matrix A of size $l \times p$ with $l \leq p$. The complexity of linear system resolution (e.g., by Gaussian elimination) is polynomial, and it is exponential for SAT solving. So, we also implemented the contextuality test (i.e., whether a configuration is contextual or not) of subspaces by linear system resolution, with Gaussian elimination optimized for sparse matrices, as implemented in the function `lu_solve` of the SpaSM tool (Bouillaguet, 2017), to compare its efficiency in practice with SAT solving with `kissat_gb`, when computing times are neither negligible nor too long for this comparison.

For subspaces of dimension $k = 2$ and $N = 5$ qubits, the computation time is 3 s for `kissat_gb` and 40 s for SpaSM. For $k = 3$, it is 45 s for `kissat_gb` and 150 s for SpaSM. This suggests that SAT solving is faster than Gaussian elimination to check non-contextual configurations. However, for contextual configurations, SpaSM appears to be faster. For $N = 7$, SpaSM validates the contextuality of an hyperbolic quadric in 21 s, against 32 s for `kissat_gb`, and the contextuality of an elliptic quadric in 14 s, against 31 s for `kissat_gb`.

4. Computational Results

The results provided by the C program are summarized in Table 1, where N is the number of qubits, # contexts is the number of contexts (i.e., the number of rows of A and E), # neg. contexts is the number of contexts with negative sign among them, # obs. is the number of observables (i.e., the number of columns of A), d is the contextuality degree, and $D(N)$ is the number of N -qubits doilies, given in Muller *et al.* (2022, Section 3).

Results are grouped by family of configurations (first column), and # config^o is the number of configurations in this family. The numbers of subspaces computed by the C program for any N and k match those given by (2). The column C/NC indicates whether all the configurations in this family are Contextual or Not Contextual. Since the generators of W_2 are its lines, their properties given in the first block for lines are not repeated in the block for generators.

Table 1 significantly extends Table 2 in de Boutray *et al.* (2022), in which the bounds for the contextuality degree d for lines with $N = 3, 4, 5$ qubits should be, according to Cabello (2010), the numbers 90, 1908, and 35400 of negative contexts, instead of the numbers 135, 1539, and 16155 of the corresponding bound b , with the notations of Section 2.1.

For a quicker orientation, the new results and improved bounds, detailed in the rest of this section, are shown in the **bold font style** in Table 1.

4.1 Results for subspaces

For lines with 3 qubit observables, the C program found a valuation with 63 invalid constraints, and no valuation with 62 invalid constraints or less, thus justifying that the contextuality degree

Table 1. Known and **new** results for the contextuality degree of various configurations

Configuration	N	# neg. contexts	# config ^o	# contexts	# obs.	C/NC	d
Lines ($k = 1$)	2	3	1	15	15	C	3
Lines ($k = 1$)	3	90	1	315	63	C	63 (90)
Lines ($k = 1$)	4	1908	1	5355	255	C	≤ 2268
Lines ($k = 1$)	5	35 400	1	86 955	1023	C	≤ 40391
Subspaces ($k = 2$)	4	4752	1	11 475	255	NC	0
Subspaces ($k = 2$)	5	358 560	1	782 595	1023	NC	0
Subspaces ($k = 2$)	6	24 330 240	1	50 868 675	2047	?	?
Subspaces ($k = 2$)	7	1 602 215 424	1	3 268 162 755	4095	?	?
Subspaces ($k = 3$)	5	0	1	782 595	1023	NC	0
Subspaces ($k = 3$)	6	0	1	213 648 435	2047	NC	0
Subspaces ($k = 4$)	6	0	1	103 378 275	2047	NC	0
Generators ($k = N - 1$)	3	54	1	135	63	NC	0
Generators ($k = N - 1$)	4	0	1	2295	255	NC	0
Generators ($k = N - 1$)	5	0	1	75 735	1023	NC	0
Generators ($k = N - 1$)	6	0	1	4 922 775	2047	NC	0
Generators ($k = N - 1$)	7	0	1	635 037 975	4095	NC	0
Doilies	[2..5]	[3..12]	$D(N)$	15	15	C	3
Mermin–Peres squares	[2..5]	1, 3 or 5	$10 \times D(N)/4^{N-2}$	6	9	C	1

Table 1. Continued

Configuration	N	# neg. contexts	# config ^o	# contexts	# obs.	C/NC	d
Two-spreads	[2..5]	1, 3, 5, 7 or 9	$6 \times D(N)$	10	15	C	1
Hyperbolics	2	1 or 3	10	6	9	C	1
Hyperbolics	3	27 or 39	36	105	35	C	21
Hyperbolics	4	532	81	1575	135	C	$\leq 500^1$
Hyperbolics	4	604	54	1575	135	C	$\leq 500^1$
Hyperbolics	4	612	1	1575	135	C	$\leq 517^1$
Hyperbolics	5	9420, 9852 or 9900	528	23 715	527	C	$\leq 10878^1$
Elliptics	2	0	6	0	5	C	N/A
Elliptics	3	9 or 13	28	45	27	C	9
Elliptics	4	360	12	1071	119	C	$\leq 351^1$
Elliptics	4	384	108	1071	119	C	$\leq 363^1$
Elliptics	5	7860, 7876 or 8020	496	19 635	495	C	$\leq 9169^1$
Perpsets	2	0 or 1	15	3	7	NC	0
Perpsets	3	0, 4 or 6	63	15	31	NC	0
Perpsets	4	0, 16, 24 or 28	255	63	127	NC	0
Perpsets	5	0 ... 120	1023	255	511	NC	0
Perpsets	6	0 ... 496	4095	1023	2047	NC	0
Perpsets	7	0 ... 2016	16 383	4095	8191	NC	0

¹ These numbers are found at least for one of the configurations.

is 63. This exact value is lower than the previously known bound, which was the number 90 of negative lines. For four and five qubits, the contextuality checks succeed, but the time to compute the contextuality degree is too high when the variable i in Algorithm 2 is initialized with the number $|C^+|$ of positive contexts (Line 2). When initializing it with the total number $|C|$ of contexts, we obtained at best the bounds 2 268 and 40 391 for the contextuality degree for 4 and 5 qubits. These bounds are not interesting, since they are higher than the number of negative contexts.

For planes ($k = 2$), the contextuality degree has been computed up to five qubits and is always 0. Table 1 also shows the number of negative planes for six and seven qubits that we were able to generate. However, we could not compute their contextuality degree, because the input files for bc2cnf and SpaSM are too large.

The totally isotropic subspaces of dimension k of W_N computed for $(k, N) = (3, 4), (3, 5), (3, 6), (4, 5), (4, 6), (5, 6),$ and $(6, 7)$ appear to be positive. These results suggest that this positivity property might hold for all $N > k \geq 3$, with the consequence that the configuration whose contexts are all these subspaces for given k and N is non-contextual. After further examination, this property indeed holds. We state it as Proposition 3 and prove it in Section 5.2.

4.2 Results for perpsets, quadrics, doilies, Mermin–Peres squares, and two-spreads

For quadrics and perpsets, the C program gives the same contextuality answers as in de Boutray et al. (2022). Moreover, it additionally checks that all perpsets with 6 and 7 qubits are non-contextual.

For N qubits, there seems to be N possible numbers of negative lines in a perpset (de Boutray et al., 2022). These numbers seem to be four times the number of negative lines in a perpset of $N - 1$ qubits, plus an additional number that seems to match the OEIS A006516 sequence (<https://oeis.org/A006516>).

The case of *three-qubit* quadrics is particularly interesting in the sense that, in addition to reconfirming their exact degree of contextuality found earlier, we can also explicitly see the geometric patterns formed by corresponding invalid (or unsatisfiable) constraints. Thus, for each of 28 elliptic quadrics living in $\mathscr{W}(5, 2)$, we found that 9 invalid constraints form a set of 9 pairwise disjoint lines partitioning the set of points of the quadric, that is, it is a *spread of lines*. Similarly, for each of 36 hyperbolic quadrics living in $\mathscr{W}(5, 2)$, the geometry formed by the 21 unsatisfiable contexts is isomorphic to that depicted in Figure 2. This geometry is underpinned by the *Heawood graph* (Heawood, 1890). This remarkable bipartite graph has 14 vertices and 21 edges, being isomorphic to the point-line incidence (or Levi) graph of the Fano plane; in Figure 2, the seven big empty circles correspond to the seven points of the Fano plane, while the seven big filled circles correspond to the seven lines, with an edge joining an empty vertex to a filled vertex iff the corresponding point lies on the corresponding line. On a hyperbolic quadric, both seven-sets can be labeled by the points/observables of two distinct disjoint Fano planes lying on the quadric in such a way that any two observables joined by an edge commute and thus define the line/context whose the third observable (represented by a smaller gray-shaded circle) is the product of the two. Note that, as in the case of elliptic quadrics, the 21 lines entail all the 35 points/observables of the quadric.

Concerning Mermin–Peres squares, the table just restates a well-known result proved in Holweck and Saniga (2017) that each grid is contextual once embedded in an arbitrary multi-qubit symplectic polar space of order 2. Similarly, all multi-qubit doilies have already been shown to be contextual for any N , their degree of contextuality being always 3 (Muller et al., 2022, Proposition 1). Contextuality of two-spreads is an important novelty of this work, their degree of contextuality being proved (see Section 5.5) to be 1 irrespectively of the value of the rank of the ambient symplectic space.

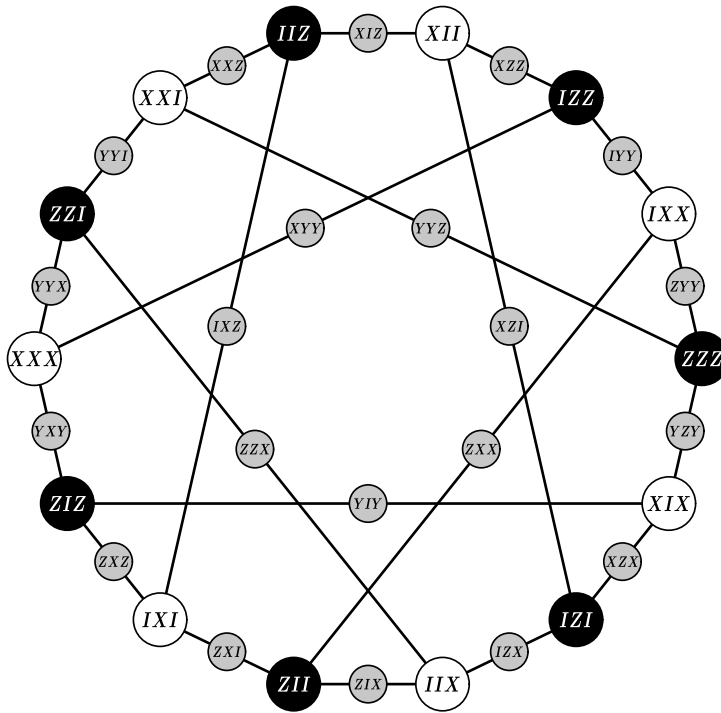


Figure 2. An illustration of the point-line configuration formed by 21 invalid constraints of the particular three-qubit hyperbolic quadric that consists solely of symmetric observables.

The C program took on average 10 min to compute the contextuality degree 21 of 1 hyperbolic quadric of 3 qubits, with the default SAT solver `minisat`. Almost the entirety of the time is taken checking the unsatisfiability of the last system. This is the longest computation time, compared to perpsets and elliptics. For this reason, we checked the top three SAT solvers of 2021 (<https://github.com/simewu/top-SAT-solvers-2021>) and found out that `kissat_gb` was the fastest for our problem. Indeed, it took an average of 10 s to find the contextuality degree of an hyperbolic of three qubits. Thus, the time to compute the contextuality degree of all the hyperbolics for three qubits was reduced down to 5 min and to a few seconds for elliptics and perpsets.

The results are the same as the ones in de Boutray et al. (2022). However, as with the Magma implementation, it does not seem possible to compute in the same way the contextuality degree of configurations with more than three qubits. From our computations up to now, it comes that for four qubits the contextuality degree of elliptics is at most 351 for one of those with 360 negative lines, at most 363 for one of those with 384 negative lines. It is at most 500 for one of the hyperbolics with 532 or 604 negative lines and at most 517 for the single one with 612 negative lines. For five qubits, when starting from the number of positive contexts, the times to compute the contextuality degree of hyperbolics and elliptics are too high. When starting from the total number of contexts, the best bounds 10 878 and 9 169 obtained are not interesting, since they exceed the number of negative contexts of hyperbolics and elliptics, respectively.

5. Contextuality-Related Properties

This section presents contextuality-related properties holding for all numbers of qubits beyond a certain known threshold.

Table 2. Illustrative example for the proofs of Proposition 3 and Lemma 4

i	$i_3 i_2 i_1 i_0$	b^i	$ b^i _3$	$ b^{2^i} _3, b^{2^{i+1}} _3$	$ b^i _2$	$ b^{2^i} _2, b^{2^{i+1}} _2$	$ b^i _1$	$ b^{2^i} _1, b^{2^{i+1}} _1$	$ b^i _0$	$ b^{2^i} _0, b^{2^{i+1}} _0, b^{2^i} \cdot b^{2^i} _0, b^{2^i} \cdot b^{2^i} \cdot b_{0 0}$
0	0000	IIII	I		I		I		I	
1	0001	$b_0 = IYZ$	I	I.I = I	I	I.I = I	Y	I.Y = Y	Z	
2	0010	$b_1 = IXXX$	I		X	X.X = I	X		X	
3	0011	$b_1, b_0 = IXZY$	I	I.I = I	X		Z	X.Z = -iY	Y	X.Y.Y.X = I
4	0100	$b_2 = XZXY$	X	X.X = I	Z	Z.Z = I	X	X.Z = -iY	Y	
5	0101	$b_2, b_0 = -XZZX$	X		Z		Z		X	
6	0110	$b_2, b_1 = XYIZ$	X	X.X = I	Y	Y.Y = I	I	I.Y = Y	Z	
7	0111	$b_2, b_1, b_0 = XYIY$	X		Y		Y		I	
8	1000	$b_3 = ZIXX$	Z	Z.Z = I	I	I.I = I	X	X.Z = -iY	X	
9	1001	$b_3, b_0 = ZIZY$	Z		I		Z		Y	
10	1010	$b_3, b_1 = ZXII$	Z	Z.Z = I	X	X.X = I	I	I.Y = Y	I	I.Z.Z.I = I
11	1011	$b_3, b_1, b_0 = ZXYZ$	Z		X		Y		Z	
12	1100	$b_2, b_2 = -YZIZ$	Y	Y.Y = I	Z	Z.Z = I	I	I.Y = Y	Z	
13	1101	$b_2, b_2, b_0 = -YZYI$	Y		Z		Y		I	
14	1110	$b_2, b_2, b_1 = YYXY$	Y	Y.Y = I	Y	Y.Y = I	X	X.Z = -iY	Y	
15	1111	$b_2, b_2, b_1, b_0 = -YYZX$	Y		Y		Z		X	
			I^8		I^8		$Y^4, (-iY)^4 = I$		$(I.Z).I.(Z.I).(X.Y).I.(Y.X) = I$	
			trivial		trivial		case 1, with $U = X$		case 2, with $r = (0, 1, 1)$ and $q = 1$	

5.1 Perpsets

Proposition 2. All perpsets are non-contextual.

Proof. Remember that the perpset of the point $p \in W_N$ is the configuration of the points q commuting with p whose contexts are the lines of W_N containing p . Consequently, any point $q \neq p$ in the perpset of p belongs to the unique line $\{p, q, p + q\}$. Thus, the two variables v_q and v_{p+q} (other than the variable v_p associated with p) in the sign constraint $v_p + v_q + v_{p+q} = e$ of the line $\{p, q, p + q\}$ appear in no other sign constraint. Whatever the values of v_p and e , it is always possible to find a value for v_q and v_{p+q} to satisfy this constraint $v_p + v_q + v_{p+q} = e$. So, the entire system of sign constraints is always solvable and all perpsets are non-contextual. □

5.2 Totally isotropic subspaces of dimension $k \geq 3$

Proposition 3. For $N > k \geq 3$, all totally isotropic subspaces of W_N of dimension k are positive. Consequently, the quantum configuration whose contexts are the totally isotropic subspaces of W_N of dimension k is non-contextual.

Proof. A totally isotropic subspace of W_N is positive if the phase of the product of the elements in the N -qubit Pauli group that are bijectively associated with its points is 1. Thus, after introducing some notations, we reformulate and formalize the positivity property with the matrix product in this (non-commutative) group.

Let $M = \{I, X, Y, Z\}$. Let $|\cdot|$ denote the norm on the Pauli group $\mathcal{P}^{\otimes N} = \{1, -1, i, -i\} \times M^{\otimes N}$, defined as phase removal by $|pa| = a$ for any phase $p \in \{1, -1, i, -i\}$ and any $a \in M^{\otimes N}$. Let us denote by $|\cdot|$ the binary operation on $M^{\otimes N}$ such that, for all $a, b \in M^{\otimes N}$, $a |\cdot| b = |a \cdot b|$. (Here, the dot “.” denotes the matrix product in $\mathcal{P}^{\otimes N}$.) For ι in \mathbb{F}_2 (whose elements are the binary digits 0 and 1) and a in $M^{\otimes N}$, let a^ι be the multiplication by a scalar defined by $a^0 = I^{\otimes N}$ and $a^1 = a$. With this multiplication by a scalar and the product $|\cdot|$, it is easy to check that $M^{\otimes N}$ is a vector space (of dimension $2N$) over \mathbb{F}_2 .

A totally isotropic subspace of W_N of (projective) dimension k is bijectively associated with a vector subspace S of (vectorial) dimension $k + 1$ of $M^{\otimes N}$, without its neutral element $I^{\otimes N}$. Since multiplying with this neutral element does not change the value of the product of all the elements of S , the totally isotropic subspace of W_N is positive if and only if the matrix product (with “.”) of all the observables in S equals $I^{\otimes N}$.

We illustrate the notations and proof steps with the explicit example in Table 2, for $k = 3$ and $N = 4$.

For $m \geq 0$, the natural number $i = i_m 2^m + \dots + i_0 2^0$, with $i_m, \dots, i_0 \in \mathbb{F}_2$, is identified with the tuple (i_m, \dots, i_0) of its binary digits. For $m = 3$, these 16 numbers $i \in [0..15]$ and their binary encoding $i_3 \dots i_0$ are, respectively, listed in the first and second column of Table 2. For any tuple $b = (b_l, \dots, b_u)$ of N -qubit observables and any tuple $i = (i_l, \dots, i_u)$ of binary digits with the same length as b , let b^i denote the matrix product $b_l^{i_l} \dots b_u^{i_u}$ in this order. (Despite the multiplicative notation, it is a linear combination of the elements of b , with 0 or 1 coefficients.)

Let $b = (b_k, \dots, b_0)$ be a basis of S . Its $k + 1$ elements are independent and mutually commuting N -qubit observables, chosen without phase. In Table 2, the basis b is $(ZIXX, XZXY, IXXX, IIYZ)$. The value of each b^i is displayed in the third column. The basis vectors b_0, b_1, b_2 , and b_3 , respectively, appear in the rows of this column indexed by $i = 1, 2, 4$ and 8 . With the former conventions and notations, the elements of S are the norms of all the linear combinations b^i for $0 \leq i \leq 2^{k+1} - 1$. So, formally, the positivity property to prove is

$$\prod_{0 \leq i < 2^{k+1}} |b^i| = I^{\otimes N}, \tag{8}$$

where $\prod_{\ell \leq i \leq u} a_i$ denotes the generalized matrix product $a_\ell \dots a_u$ of all the elements in the finite sequence $(a_i)_{\ell \leq i \leq u}$ of N -qubit observables, in this order.

For $1 \leq j \leq N$, let a_j denote the j -th qubit of the phase-free N -qubit observable $a \in M^{\otimes N}$. For $0 \leq m \leq k$, the j -th qubit of the m -th basis vector b_m is denoted $b_{m,j}$. As a direct consequence, for all s, t in $\mathcal{P}^{\otimes N}$,

$$|s.t|_j = |s|_j |t|_j. \tag{9}$$

The matrix product of all the elements of S (left-hand side of (8)) is the tensor product for all $j \in [1..N]$ of the matrix products of their j -th qubits. Formally,

$$\prod_{0 \leq i < 2^{k+1}} |b^i| = \bigotimes_{1 \leq j \leq N} \prod_{0 \leq i < 2^{k+1}} |b^i|_j.$$

So, we prove that it is $I^{\otimes N}$ as a consequence of the (stronger) fact that all the products of their j -th qubits equal I (Lemma 4), when the order of the qubit products is chosen to be the *lexicographic order* on the tuples (i_{m-1}, \dots, i_0) , corresponding to the usual order $<$ on the natural numbers they encode. Since S comes from a totally isotropic space, all its pairs of elements mutually commute, so the order of the product of all its elements (left-hand side of (8)) can be chosen to be this lexicographic order.

In Table 2, the j -th qubit $|b^i|_j$ of the elements of S are shown in Columns 4, 6, 8, and 10, for $j = 3, 2, 1$, and 0 . The matrix product of all elements in each of these columns is expected to be I . The remaining contents of Table 2 are described in the proof of Lemma 4, postponed in Appendix A to lighten the present proof, which ends here. □

Lemma 4. For $3 \leq k \leq N - 1$, let S be a vector subspace of $M^{\otimes N}$, of dimension $k + 1$, generated by a basis (b_k, \dots, b_0) of $k + 1$ independent and mutually commuting vectors without phase. Let $L = (|b^i|)_{0 \leq i < 2^{k+1}}$ be the sequence of all the elements of S in lexicographic order. Then, for all $1 \leq j \leq N$, the matrix product $\prod_{0 \leq i < 2^{k+1}} |b^i|_j$ of all the elements of the sequence of j -th qubits in L , in the same order as in L , always equals I .

5.3 Geometrical constraints and a related corollary on the sign(s) of three-dimensional subspaces

In addition to the algebraic proof of Proposition 3 presented in Section 5.2, this section provides a geometric interpretation of the positivity of every $PG(3, 2)$ of a multi-qubit W_N , for $N \geq 4$.

Proposition 5. *Let P be a $PG(3, 2)$ of a multi-qubit W_N with $N \geq 4$. Then, the following four propositions are equivalent:*

- (a) P is negative.
- (b) Each of the 56 spreads of lines of P contains an odd number of negative lines.
- (c) Through each of the 35 lines of P there pass an odd number of negative planes.
- (d) Through each of the 15 points of P there pass an odd number of negative lines.

Proof. As the observables of any subspace of W_N mutually commute, we can take any product of observables in P in any order.

(a) \Leftrightarrow (b) A spread of lines of P is a set of five pairwise disjoint lines that partition the set of points of P . Pick up a spread of lines, take first the product of the three observables on each line of the spread, and then multiply the five products obtained to get the sign of P . This space will be *negative* (i.e., the product of all the 15 observables will be equal to $-I^{\otimes N}$) iff the number of negative lines in the spread selected is *odd*. Clearly, this property must hold irrespectively of which spread of lines we select.

(a) \Leftrightarrow (c) Let us assume that the 15 points/observables of P are labeled simply as $\{a, b, c, d, e, f, g, h, i, j, k, l, m, n, o\}$, that a, b, c lie on a line and that the three planes through this line are $F_1 = \{a, b, c; d, e, f, g\}$, $F_2 = \{a, b, c; h, i, j, k\}$, and $F_3 = \{a, b, c; l, m, n, o\}$. Let us consider the following product of the products of all the points in each of these three planes:

$$(a.b.c.d.e.f.g).(a.b.c.h.i.j.k).(a.b.c.l.m.n.o). \tag{10}$$

By commutation relations and $a^2 = b^2 = c^2 = I^{\otimes N}$, this product (10) equals the product

$$a.b.c.d.e.f.g.h.i.j.k.l.m.n.o, \tag{11}$$

of all the points of P . So, P is negative iff one or all the three planes through the line in question are negative.

Again, as the sign of the space is an invariant this reasoning must hold for the planes through any line of P .

(a) \Leftrightarrow (d) Let us assume that the seven lines passing via the point/observable a are $\{a, b, c\}$, $\{a, d, e\}$, $\{a, f, g\}$, $\{a, h, i\}$, $\{a, j, k\}$, $\{a, l, m\}$, and $\{a, n, o\}$. Consider the following product of the products of all the points in these lines:

$$(a.b.c).(a.d.e).(a.f.g).(a.h.i).(a.j.k).(a.l.m).(a.n.o). \tag{12}$$

After simplification, it again equals the product (11) of all the points of P . So, P is negative iff the number of negative lines passing through a is odd.

Again, this must hold irrespectively of the reference point/observable chosen. □

As we have proved (see Proposition 3) that there are no negative $PG(3, 2)$'s in W_N , for $N \geq 4$, Proposition 5 leads to the following geometrically slanted corollary:

Corollary 6. *As a $PG(3, 2)$ of a multi-qubit W_N , $N \geq 4$ is always positive, then: a) each of its 56 spreads of lines contains an even number of negative lines; b) through each of its 35 lines there pass an even number of negative planes; and c) through each of its 15 points there pass an even number of negative lines.*

5.4 No analogs of Mermin pentagrams in the four-qubit case

Given the fact, stemming from Proposition 3, that all generators – that is, $PG(3, 2)$ s – of the four-qubit $\mathscr{W}(7, 2)$ are positive, there will be no analogs of (three-qubit) Mermin pentagrams in the four-qubit case. We illustrate this fact in Figure 3. We took a particular quadratic $\mathscr{W}(5, 2)$ having

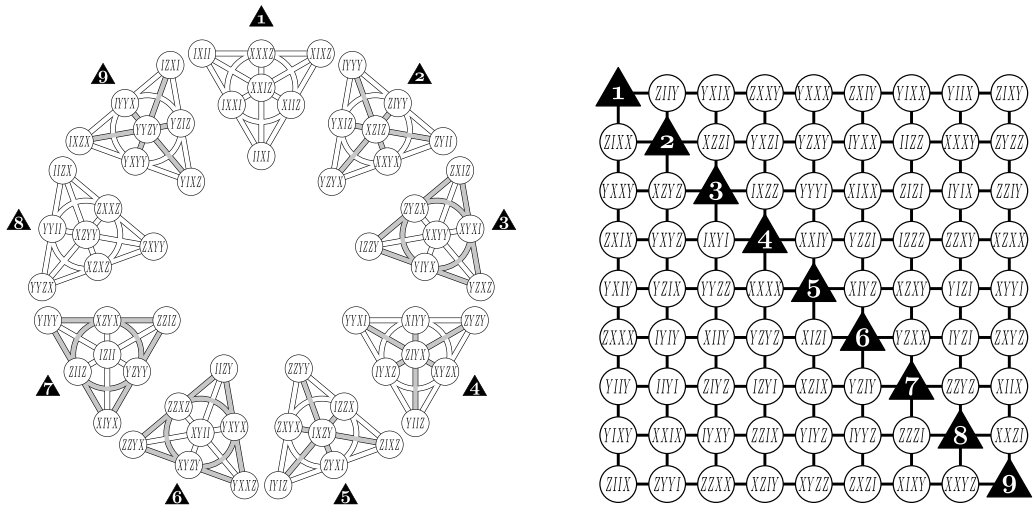


Figure 3. *Left:* A spread of planes in the selected four-qubit $\mathscr{W}(5, 2)$, with negative lines shown in gray; each plane featuring three concurrent negative lines is negative. *Right:* The associated sets of 18 contexts (9 rows and 9 columns), 2 per each plane of the spread.

42 negative planes. In this $\mathscr{W}(5, 2)$, we picked up one spread of planes; this spread features four negative planes and is illustrated on the left-hand side of the figure. Now, through each plane of $\mathscr{W}(7, 2)$ there are three $PG(3, 2)$ s, and the totality of 27 such spaces can be split into 3 sets of 9 elements each. One set has a special footing as all its $PG(3, 2)$ s pass through a common point – the pole of that $PG(6, 2)$ where our $\mathscr{W}(5, 2)$ is located in (being also the nucleus of the $\mathscr{W}(5, 2)$) – and it will be disregarded. The other two nine-element sets are similar in the sense that each of them consists of mutually disjoint $PG(3, 2)$ s. The affine parts, $AG(3, 2)$ s, of these spaces of either set, however, cover the same $(9 \times 8 =) 72$ points; this means that each of these 72 points will lie in two different $AG(3, 2)$ s. In analogy with a Mermin pentagram, these $(9 \times 2 =) 18$ $AG(3, 2)$ s will be our contexts. They are shown on the right-hand side of Figure 3; here, the two contexts originating from the same plane of the spread are arranged in the row and/or the column bearing the number of the corresponding plane. From this construction, it is clear that *irrespective* of the number of negative planes our selected spread features, there will always be an *even* number of negative contexts in our analog of a Mermin pentagram; indeed, each $PG(3, 2)$ – being always positive – that passes via a negative plane will have the corresponding $AG(3, 2)$ negative, but for each plane these $AG(3, 2)$ s come in pairs. A similar argument can be used to show that there are no higher-rank analogs of Mermin pentagrams for any $N > 3$.

5.5 Contextuality properties of two-spreads: The contextuality degree of all N -qubit two-spreads is 1

Apart from grids (aka Mermin–Peres magic squares), a multi-qubit doily hosts another prominent, yet almost virtually unknown to the quantum informational community, class of contextual configurations, the so-called two-spreads. Given a multi-qubit doily, remove from it one spread of lines while keeping all the points; what we get is a *two-spread*, that is, a (sub-)configuration having 15 points and 10 lines, with 3 points per line and 2 lines per point (see, e.g., Figure 8 of Polster (1998)). Figure 4 is an illustration of a two-spread living in a quadratic five-qubit doily.

Let us briefly recall that a “classical” contextual point-line configuration features (a) an even number of lines/contexts per point/observable and (b) an odd number of negative lines/contexts (Holweck and Saniga, 2017). We already see that a multi-qubit two-spread meets the first condition (as there are two lines per each of its points). Now we show that it also satisfies the second condition. To this end in view, we readily infer from our computer-generated

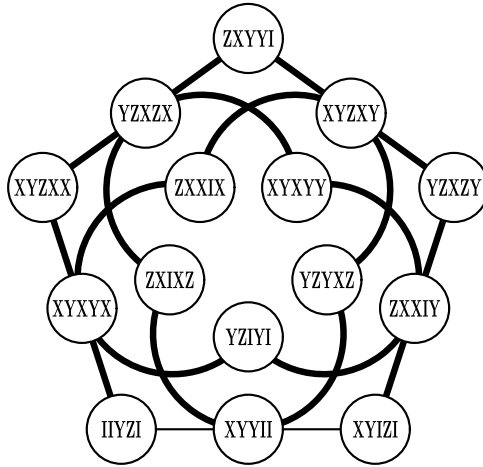


Figure 4. An example of five-qubit two-spread having nine (i.e., the maximum possible number of) negative lines (bold-faced).

results (after carefully inspecting Figure 2 of our recent paper (Muller et al., 2022)) that if a doily is endowed with an *odd* number of negative lines, each of its six spreads of lines contains an *even* number of them, whereas if a doily features an *even* number of negative lines, each of its six spreads shares an *odd* number of them. That is, removal of a spread leads in both cases to a configuration endowed with an *odd* number of negative lines, as envisaged.

The former reasoning is substantiated by our exhaustive computer-aided analysis up to $N = 5$. In W_N , for $2 \leq N \leq 5$, we picked up a representative doily from each type (defined by the signature of observables) and subtype (defined by the pattern formed by negative lines) as classified in Muller et al. (2022) and found out that all six two-spreads in it were contextual. Moreover, we also found that in each case the degree of contextuality was the same and equal to 1. In fact, by analyzing the incidence matrix of the two-spread configuration, it appears that all two-spreads are contextual and the vector E of negative lines is at Hamming distance 1 of the image of the incidence matrix. In other words, we have the following proposition:

Proposition 7. *A two-spread in an N -qubit doily is contextual for each $N \geq 2$, and its degree of contextuality is always 1.*

Proof. Consider the incidence matrix of the two-spread configuration:

$$A = \begin{pmatrix} 1 & 1 & 1 & 0 & 0 & 0 & 0 & 0 & 0 & 0 & 0 & 0 & 0 & 0 & 0 \\ 0 & 0 & 1 & 1 & 1 & 0 & 0 & 0 & 0 & 0 & 0 & 0 & 0 & 0 & 0 \\ 0 & 0 & 0 & 0 & 1 & 1 & 1 & 0 & 0 & 0 & 0 & 0 & 0 & 0 & 0 \\ 0 & 0 & 0 & 0 & 0 & 0 & 1 & 1 & 1 & 0 & 0 & 0 & 0 & 0 & 0 \\ 1 & 0 & 0 & 0 & 0 & 0 & 0 & 0 & 1 & 1 & 0 & 0 & 0 & 0 & 0 \\ 0 & 1 & 0 & 0 & 0 & 0 & 0 & 0 & 0 & 0 & 0 & 1 & 0 & 0 & 1 \\ 0 & 0 & 0 & 1 & 0 & 0 & 0 & 0 & 0 & 0 & 1 & 0 & 1 & 0 & 0 \\ 0 & 0 & 0 & 0 & 0 & 1 & 0 & 0 & 0 & 0 & 0 & 1 & 0 & 1 & 0 \\ 0 & 0 & 0 & 0 & 0 & 0 & 0 & 1 & 0 & 0 & 0 & 0 & 1 & 0 & 1 \\ 0 & 0 & 0 & 0 & 0 & 0 & 0 & 0 & 0 & 1 & 1 & 0 & 0 & 1 & 0 \end{pmatrix}.$$

The linear combinations of the rows of A span the nine-dimensional space of vectors in \mathbb{F}_2^{10} having an even number of 1s in their decomposition in the standard basis. In fact, $\text{Im}(A)$ is the space of length-10 binary vectors with an even number of 1s. Thus, any vector E representing a context evaluation with an odd number of negative lines, that is, an odd number of 1s, is at Hamming distance 1 of $\text{Im}(A)$. This proves that two-spreads are always contextual with contextuality degree 1. \square

5.6 Contextuality degree of three-qubit lines

A very instructive result in Table 1 concerns the contextuality degree of lines of W_3 . This result contradicts Lemma 3 and Figure 1 of Cabello (2010). Indeed the contextuality degree corresponds to the minimal number of constraints that cannot be satisfied by any NCHV. In Cabello (2010), it is supposed to be always equal to the number of negative lines when we consider, for a fixed N , all N -qubit observables and all lines. But the model obtained by the SAT solver was able to satisfy, in the three-qubit case, $315 - 63 = 252$ constraints instead of 235 as previously obtained. Note that this new result changes the contextuality bound experimentally tested in Holweck (2021). The experimental evaluation of Equation (6) on IBM quantum computers described in Holweck (2021) provided a result of 236, which still violates the classical bound, now known to be $b = 315 - 2 \times 63 = 189$, instead of the erroneous value $315 - 2 \times 90 = 135$.

With the C implementation of the contextuality degree algorithm 2, we managed to compute the contextuality degree of three-qubit lines. The intermediate partial solutions found had the following Hamming distances: 89, 86, 79, 72, and 63. This means that it first checked for a Hamming distance that is at most the number of negative lines, 90, and found a solution with 89 invalid constraints, and then it checked for at most 1 less invalid constraints and found 86 of them. This process was repeated until it found a configuration with 63 invalid constraints, after which the solver found no solution when asked to let at most 62 invalid constraints satisfied. Thus, the contextuality degree of the configuration of the lines of W_3 is 63.

It is worth concluding this section by mentioning that in this case we carried out several runs with the SAT solver and, strikingly, in each case the set of 63 invalid constraints/lines was found to be isomorphic to a copy of the split Cayley hexagon of order 2 when embedded classically into W_3 ; the copy for one of these sets is illustrated in Figure 5. This finding sheds a rather unexpected new light on the contextuality role of the hexagon in the three-qubit symplectic polar space discovered in Holweck *et al.* (2022) and will be treated in more detail in a separate paper.

6. Conclusion

One of the most intriguing outcomes of our work is the fact that there are no negative subspaces of dimension 3 and higher. This has a couple of interesting implications. The first one concerns Mermin–Peres squares and Mermin pentagrams. In the former case, the contexts correspond to generators of the ambient $\mathscr{W}(3, 2)$, while in the latter case the contexts represent affine parts of generators of $\mathscr{W}(5, 2)$. The non-existence of negative generators for $k \geq 3$ then simply means that there will be no higher-dimensional analogs of these two important classes of contextual configurations in polar spaces of rank 5 and higher. The second implication concerns contextuality properties of s -qubit $\mathscr{W}(2s - 1, 2)$'s living in the ambient N -qubit $\mathscr{W}(2N - 1, 2)$, for $s < N$. We have already verified that all multi-qubit doilies ($s = 2$) are contextual for any N , and that their degree of contextuality is 3 (Muller *et al.*, 2022, Proposition 1). As the next natural step, it would be vital to address the corresponding behavior of rank 3 and, especially, rank 4 polar spaces.

Next, given a multi-qubit $\mathscr{W}(2N - 1, 2)$, remove from it a spread of generators while keeping all the observables; what we get is an analog of a doily's two-spread. It would be desirable to check, at least for a few randomly selected cases, if these higher-dimensional analogs of two-spreads of a multi-qubit doily are contextual, or not.

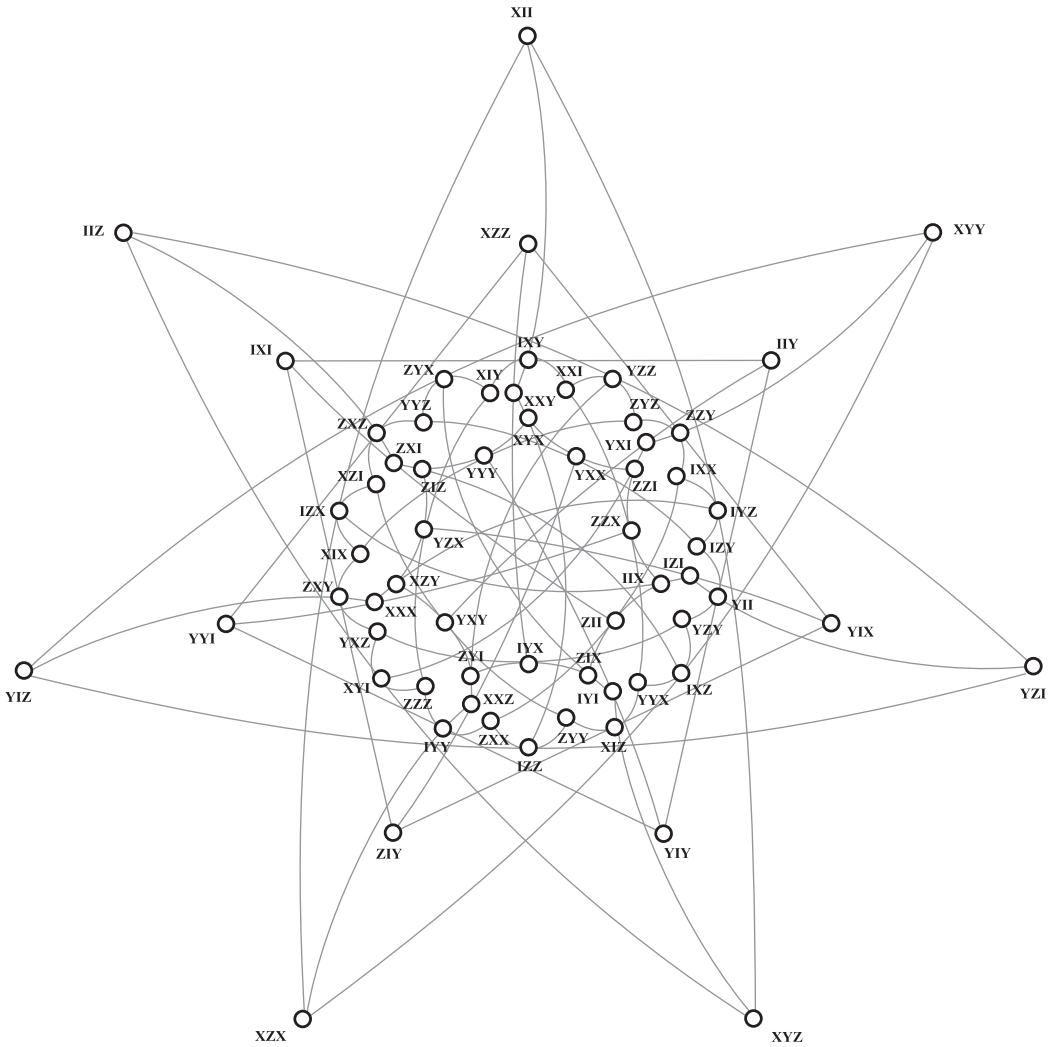


Figure 5. A classically embedded three-qubit split Cayley hexagon of order 2 that accommodates all the 63 invalid constraints for a particular solution found by the SAT solver. The graphical illustration of the hexagon is a simplified reproduction of that given in Polster et al. (2001).

A final prospective task is to address the contextuality of quadrics when instead of lines we consider their *planes* as contexts. A particular worth-deserving object in this respect is a hyperbolic quadric of the four-qubit symplectic polar space. This quadric, sometimes called the triality quadric, possesses an unexpected threefold symmetry and, in addition, it hosts 960 ovoids, each of them being related via a particular Grassmannian mapping to a spread of planes in the three-qubit polar space.

Acknowledgements. We thank Zsolt Szabó for his help with Figures 2, 3, and 4.

Financial Support. This project is supported by the PEPR integrated project EPiQ ANR-22-PETQ-0007 part of Plan France 2030, by the project TACTICQ of the EIPHI Graduate School (contract ANR-17-EURE-0002). This work also received a partial support from the Slovak VEGA grant agency, Project 2/0004/20.

Competing Interests. The authors declare no competing interests.

References

- Bouillaguet, C. (2017). *SpaSM: A Sparse Direct Solver Modulo p*, v1.2 edition. <http://github.com/cbouilla/spasm>.
- Budroni, C., Cabello, A., Gühne, O., Kleinmann, M. and Larsson, J.-Å. (2022). Kochen-Specker contextuality. *Reviews of Modern Physics* **94** 045007. <https://doi.org/10.1103/RevModPhys.94.045007>.
- Cabello, A. (2010). Proposed test of macroscopic quantum contextuality. *Physical Review A* **82** (3) 032110. <https://doi.org/10.1103/PhysRevA.82.032110>.
- Chowdhury, M., Müller, M. and You, J. (2021). A deep dive into conflict generating decisions. <https://doi.org/10.48550/arXiv.2105.04595>.
- De Boeck, M., Rodgers, M., Storme, L. and Švob, A. (2019). Cameron-Liebler sets of generators in finite classical polar spaces. *Journal of Combinatorial Theory, Series A* **167** 340–388. <https://doi.org/10.1016/j.jcta.2019.05.005>.
- de Boutray, H., Holweck, F., Giorgetti, A., Masson, P.-A. and Saniga, M. (2022). Contextuality degree of quadrics in multi-qubit symplectic polar spaces. *Journal of Physics A: Mathematical and Theoretical* **55** (47) 475301. <https://doi.org/10.1088/1751-8121/aca36f>.
- Heawood, P. (1890). Map colouring theorems. *The Quarterly Journal of Mathematics, Oxford Series* **24** 322–339.
- Holweck, F. (2021). Testing quantum contextuality of binary symplectic polar spaces on a noisy intermediate scale quantum computer. *Quantum Information Processing* **20** (7) 247. <https://doi.org/10.1007/s11128-021-03188-9>.
- Holweck, F., de Boutray, H. and Saniga, M. (2022). Three-qubit-embedded split Cayley hexagon is contextuality sensitive. *Scientific Reports* **12** (8915). <https://doi.org/10.1038/s41598-022-13079-3>.
- Holweck, F. and Saniga, M. (2017). Contextuality with a small number of observables. *International Journal of Quantum Information* **15** (04) 1750026. <https://doi.org/10.1142/S0219749917500265>.
- Junttila, T. A. and Niemelä, I. (2000). Towards an efficient tableau method for Boolean circuit satisfiability checking. In *Computational Logic – CL 2000*, Berlin, Heidelberg. Springer Berlin Heidelberg, 553–567. https://doi.org/10.1007/3-540-44957-4_37.
- Lévay, P. and Szabó, Z. (2017). Mermin pentagrams arising from Veldkamp lines for three qubits. *Journal of Physics A: Mathematical and Theoretical* **50** (9) 095201. <https://doi.org/10.1088/1751-8121/aa56aa>.
- Mermin, N. D. (1993). Hidden variables and the two theorems of John Bell. *Reviews of Modern Physics* **65** 803–815. <https://doi.org/10.1103/RevModPhys.65.803>.
- Muller, A., Saniga, M., Giorgetti, A., De Boutray, H. and Holweck, F. (2022). Multi-qubit doilies: Enumeration for all ranks and classification for ranks four and five. *Journal of Computational Science* **64** 101853. <https://doi.org/10.1016/j.jocs.2022.101853>.
- Peres, A. (1990). Incompatible results of quantum measurements. *Physics Letters A* **151** (3) 107–108. [https://doi.org/10.1016/0375-9601\(90\)90172-K](https://doi.org/10.1016/0375-9601(90)90172-K).
- Planat, M., Saniga, M. and Holweck, F. (2013). Distinguished three-qubit “magicity” via automorphisms of the split Cayley hexagon. *Quantum Information Processing* **12** (7) 2535–2549. <https://doi.org/10.1007/s11128-013-0547-3>.
- Polster, B. (1998). Pretty pictures of geometries. *Bulletin of the Belgian Mathematical Society – Simon Stevin* **5**(2/3) 417–425. <https://doi.org/10.36045/bbms/1103409021>.
- Polster, B., Schroth, A. E., and Van Maldeghem, H. (2001). Generalized flatland. *The Mathematical Intelligencer* **23** (4) 33–47. <https://doi.org/10.1007/BF03024601>.
- Saniga, M. (2021). A class of three-qubit contextual configurations located in Fano pentads. *Mathematics* **9** (13). <https://doi.org/10.3390/math9131524>.
- Saniga, M., de Boutray, H., Holweck, F. and Giorgetti, A. (2021). Taxonomy of polar subspaces of multi-qubit symplectic polar spaces of small rank. *Mathematics* **9** (18) 2272. <https://doi.org/10.3390/math9182272>.
- Saniga, M. and Lévay, P. (2012). Mermin’s pentagram as an ovoid of PG(3, 2). *Europhysics Letters* **97** (5) 50006. <https://doi.org/10.1209/0295-5075/97/50006>.
- Saniga, M., Planat, M., Pracna, P. and Havlicek, H. (2007). The Veldkamp space of two-qubits. *SIGMA. Symmetry, Integrability and Geometry: Methods and Applications* **3** (075) 7. <https://doi.org/10.3842/SIGMA.2007.075>.

Appendix A. Proof of Lemma 4

Proof. We still write $\prod_{0 \leq i < 2^m}$ for the product in the lexicographic order or sometimes use the more compact notation $\prod_{|i|=m}$, where $|i|$ denotes the length of the tuple i . Let us prove that the product in lexicographic order of the j -th qubit of the norm of all linear combinations of length $|i| = k + 1$ of the basis vectors, that is, of all elements of S , equals the identity matrix. Formally,

$$\prod_{|i|=k+1} |b^i\rangle_j = I \quad (13)$$

for all $1 \leq j \leq N$.

If i is the k -tuple (i_k, \dots, i_1) , let $2i$ denote the $(k + 1)$ -tuple $(i_k, \dots, i_1, 0)$ and $2i + 1$ denote the $(k + 1)$ -tuple $(i_k, \dots, i_1, 1)$. For two tuples i and i' of bits (in \mathbb{F}_2) with the same length, let $i \oplus i'$ denote the bitwise addition (“exclusive or”) of their bits. From these notations, it comes that $2i \oplus 2i' = 2(i \oplus i')$.

By associating each $|b^{2i}|_j$ with its lexicographic successor $|b^{2i+1}|_j$ in the product, we get

$$\prod_{|i|=k+1} |b^i|_j = \prod_{|i|=k} (|b^{2i}|_j \cdot |b^{2i+1}|_j)$$

for $k \geq 1$. Since $b^{2i+1} = b^{2i} \cdot b_0$ and $b^{2i} \cdot b^{2i} = I^{\otimes N}$, all products $(|b^{2i}|_j \cdot |b^{2i+1}|_j)$ equal $b_{0,j}$ multiplied by some complex phase that will be precised below (in Table 2, this product is shown in Columns 5, 7, 9 and 11). This is a key property for the end of the proof, because the product of all these $b_{0,j}$ with their phase commute, which allows us to re-order them in any order, until showing that the product of all these phases is 1.

A trivial case is when $b_{0,j} = I$. It is illustrated by Columns 4–7 of Table 2, for $j = 2$ and $j = 3$. In this case all the products $(|b^{2i}|_j \cdot |b^{2i+1}|_j)$ of two consecutive qubits equal I , as detailed below:

$$|b^{2i}|_j \cdot |b^{2i+1}|_j = |b^{2i}|_j \cdot |b^{2i} \cdot b_0|_j = |b^{2i}|_j \cdot |b^{2i}|_j \cdot |b_0|_j = |b^{2i}|_j \cdot |b^{2i}|_j \cdot I = (|b^{2i}|_j)^2 = I.$$

Thus, the complete product also equals I . Apart from this trivial case, the following two complementary cases can be considered.

Case 1: Consider first the case when the inequality

$$|b^{2r}|_j \neq b_{0,j} \tag{14}$$

holds for all tuples of coefficients r of length $|r| = k$. This case is illustrated by Columns 8–9 of Table 2, for $j = 1$ and $b_{0,1} = Y$.

Let $i = (i_k, \dots, i_1)$ be any tuple of binary coefficients of length $|i| = k$. The inequality (14) with $r = 0$ implies that $b_{0,j}$ is different from I . So, the set $\{X, Y, Z\}$ of Pauli matrices is composed of $b_{0,j}$ and the other two Pauli matrices, hereafter denoted by U and V . For instance, in Columns 8–9 of Table 2, for $j = 1$, $b_{0,1} = b_{0,j} = Y$, so U can be X and V can be Z .

Now, assume that there are two tuples i and i' of binary coefficients of length k such that $|b^{2i}|_j = U$ and $|b^{2i'}|_j = V$. Then $|b^{2(i \oplus i')}|_j = |b^{2i \oplus 2i'}|_j = |b^{2i} \cdot b^{2i'}|_j = \left| |b^{2i}|_j \cdot |b^{2i'}|_j \right| = |U \cdot V| = b_{0,j}$, which contradicts the inequality (14). Consequently, there is a unique Pauli matrix, different from $b_{0,j}$, hereafter assumed to be U without loss of generality, such that the j -th qubit of each vector $|b^{2i}|_j$ with $|i| = k$ is either I or U . For instance, in Columns 8–9 of Table 2, U is X . It follows that any pair $(|b^{2i}|_j, |b^{2i+1}|_j) = (|b^{2i}|_j, |b^{2i} \cdot b_0|_j)$ of consecutive j -th qubits whose first element comes from a linear combination without b_0 is either $(I, b_{0,j})$ (for $i = 000, 011, 101,$ and 110 in Table 2) or $(U, |U \cdot b_{0,j}|_j)$ (for $i = 001, 010, 100,$ and 111 in Table 2, gray cells in Column 9).

The sets of pairs in these two cases are in one-to-one correspondence according to the involution $W \mapsto |U \cdot W|$, so their cardinality is half the total cardinality, that is, $2^k/2 = 2^{k-1}$.

In the first case, $|b^{2i}|_j \cdot |b^{2i+1}|_j = I \cdot b_{0,j} = b_{0,j}$, without phase. In the second case, $|b^{2i}|_j \cdot |b^{2i+1}|_j = U \cdot |U \cdot b_{0,j}|_j = U \cdot |\pm i V|$, because the product of two distinct Pauli matrices always yields the third one, which is V here, up to a phase which is either i or $-i$. Finally, $|b^{2i}|_j \cdot |b^{2i+1}|_j = U \cdot V = p \cdot b_{0,j}$ for the same reason, with the same phase p among i and $-i$ for all these products. For instance, this phase p is $-i$ in the gray cells in Column 9 of Table 2.

By separating the complete product along these two cases, it comes

$$\begin{aligned} \prod_{|i|=k+1} |b^i|_j &= \prod_{|i|=k} |b^{2i}|_j \cdot |b^{2i+1}|_j = \left(\prod_{|i|=k, |b^{2i}|_j=I} |b^{2i}|_j \cdot |b^{2i+1}|_j \right) \left(\prod_{|i|=k, |b^{2i}|_j=U} |b^{2i}|_j \cdot |b^{2i+1}|_j \right) \\ &= \left(\prod_{|i|=k, |b^{2i}|_j=I} b_{0,j} \right) \left(\prod_{|i|=k, |b^{2i}|_j=U} \bar{b}_{0,j} \right) = p^{2^{k-1}} \left(\prod_{|i|=k} b_{0,j} \right) = (\pm i)^{2^{k-1}} b_{0,j}^k = 1 \ I = I \end{aligned}$$

when $k \geq 3$.

Case 2: Finally, consider the complementary case when there is some tuple of coefficients $r \neq 0$ of length $|r| = k$ such that $|b^{2r}|_j = b_{0,j}$. This case is illustrated by Columns 10-11 in Table 2, with $j = 0$ and $r = 011$, since $|b^{0110}|_0 = b_{0,0} = Z$ in this example ($r = 110$ could be another valid choice).

In $r = (r_{k-1}, \dots, r_0) \neq 0$, let $0 \leq q < k$ be any non-zero coefficient ($r_q = 1$). For instance, since $r = (0, 1, 1)$ in Table 2 for $j = 0$, let us choose $q = 1$ ($q = 0$ would also hold) in this example. Let $R_0 = \{i \in [0..2^k - 1] \mid i_q = 0\}$ be the subset of numbers in $[0..2^k - 1]$ whose q -th bit is the opposite of the q -th bit $r_q = 1$ in r . Then, R_0 and $([0..2^k - 1] - R_0)$ partition $[0..2^k - 1]$ into two equal subsets, in bijection according to the involution $i \mapsto r \oplus i$. For instance, in Table 2, R_0 is $\{000, 001, 100, 101\}$.

The product $\prod_{|i|=k} |b^{2i}|_j \cdot |b^{2i+1}|_j$ is re-organized according to R_0 and simplified as follows:

$$\begin{aligned} \prod_{|i|=k+1} |b^i|_j &= \prod_{|i|=k} |b^{2i}|_j \cdot |b^{2i}.b_0|_j = \left(\prod_{|i|=k, i_q=0} |b^{2i}|_j \cdot |b^{2i}.b_0|_j \right) \left(\prod_{|i|=k, i_q=1} |b^{2i}|_j \cdot |b^{2i}.b_0|_j \right) \\ &= \left(\prod_{|i|=k, i_q=0} |b^{2i}|_j \cdot |b^{2i}.b_0|_j \right) \left(\prod_{|i|=k, i_q=0} |b^{2(r \oplus i)}|_j \cdot |b^{2(r \oplus i)}.b_0|_j \right) \\ &= \left(\prod_{|i|=k, i_q=0} |b^{2i}|_j \cdot |b^{2i}.b_0|_j \cdot |b^{2r}.b^{2i}|_j \cdot |b^{2r}.b^{2i}.b_0|_j \right). \end{aligned}$$

For instance, in Table 2, for $i = 001$, the subproduct $|b^{2i}|_j \cdot |b^{2i}.b_0|_j \cdot |b^{2r}.b^{2i}|_j \cdot |b^{2r}.b^{2i}.b_0|_j$ in this product is

$$\begin{aligned} |b^{0010}|_0 \cdot |b^{0010}.b_0|_0 \cdot |b^{0110}.b^{0010}|_0 \cdot |b^{0110}.b^{0010}.b_0|_0 &= X \cdot |X.Z| \cdot |Z.X| \cdot |Z.X.Z| \\ &= X.(Y.Y).X = X.(I).X = I. \end{aligned}$$

This reduction to I holds in all generality, as detailed below. From (9) and commutation relations, it comes that

$$|b^{2r}.b^{2i}|_j = \left| |b^{2r}|_j \cdot |b^{2i}|_j \right| = \left| b_{0,j} \cdot |b^{2i}|_j \right| = \left| |b^{2i}|_j \cdot b_{0,j} \right| = |b^{2i}.b_0|_j$$

so

$$\prod_{|i|=k+1} |b^i|_j = \left(\prod_{|i|=k, i_q=0} |b^{2i}|_j \cdot (|b^{2i}.b_0|_j)^2 \cdot |b^{2r}.b^{2i}.b_0|_j \right) = \left(\prod_{|i|=k, i_q=0} |b^{2i}|_j \cdot |b^{2r}.b^{2i}.b_0|_j \right).$$

Similarly,

$$|b^{2r}.b^{2i}.b_0|_j = \left| |b^{2r}|_j \cdot |b^{2i}|_j \cdot b_{0,j} \right| = \left| b_{0,j} \cdot |b^{2i}|_j \cdot b_{0,j} \right| = \left| b_{0,j}^2 \cdot |b^{2i}|_j \right| = |b^{2i}|_j$$

so

$$\prod_{|i|=k+1} |b^i|_j = \prod_{|i|=k, i_q=0} \left(|b^{2^i}|_j \right)^2 = \prod_{|i|=k, i_q=0} I = I$$

that completes the proof. □